Modelling the morphology of minerals by computer

A.L. ROHL* AND D.H. GAY

The Royal Institution of Great Britain, 21 Albemarle Street, London, W1X 4BS, UK

Abstract

A new computer code (MARVIN) has been developed for the simulation of surfaces and interfaces. The models and methodologies employed within the program are briefly discussed. One application of the code, calculating crystal morphologies, is explored using zircon, quartz and α-Al_2O_3 as examples. The new code enables the use of covalent type force fields and the effect of surface relaxation on the growth morphology to be calculated for the first time. It is found that relaxation does affect the attachment energy but not by a large enough amount to significantly change the growth morphology for the three examples discussed here. Finally, the calculated surface relaxation for the basal plane of α-Al_2O_3 is found to be in complete agreement with Hartree-Fock *ab initio* calculations, verifying that the potentials, which are derived from bulk properties, transfer well to this surface.

KEYWORDS: morphology, MARVIN, modelling, zircon, quartz, α-Al_2O_3, corundum.

Introduction

MORPHOLOGICAL prediction, based on the internal structure of a compound, has enjoyed many decades of active study. Initial approaches were based solely on the interplanar spacings, d_{hkl}, of the different crystal faces, with the lowest growth rates occurring at the faces with the greatest d_{hkl} (Friedel, 1907; Bravais, 1913). Donnay and Harker (1937) improved this simple idea when they took account of the symmetry of a crystal by reducing the d_{hkl} growth slices at faces containing a screw axis or glide plane, since the slice at these faces can be reduced into identical sub-slices. The presence of these symmetry elements can be easily detected by looking at the extinction conditions in the X-ray reflections, and is determined solely by the space group of the crystal. These arguments take no account of the detailed structure or energetics of a compound.

Hartman and Perdok (1955*a*) revolutionised this field by considering the role of the intermolecular forces in crystallization. They classified crystal faces into three groups depending on the number of Periodic Bond Chains (PBCs) in the growth slice, where a PBC is an uninterrupted chain of nearest neighbour interactions. A slice with two or more PBCs is an F face, those with one PBC are S faces and the rest are K faces. They proposed that only F faces can grow according to a layer mechanism, with the other two having a continuous mode of growth. Thus the growth of F faces will be slow and therefore they will be the most important morphologically. They later proposed (Hartman and Bennema, 1980) that the *attachment energy* (the energy per molecule released when a new slice of depth d_{hkl} is attached to the crystal face, E_{att}) be proportional to the growth rate and hence inversely proportional to its morphological importance. Again the depth of the slice is reduced at faces containing a screw axis or glide plane. The relationship between the attachment energy and the classification of faces by PBC analysis can be perceived in the relationship

$$E_{cr} = E_{sl}(hkl) + E_{att}(hkl) \quad (1)$$

where $E_{sl}(hkl)$ is the energy between all the ions within the slice *hkl* (slice energy) and E_{cr} is the energy of the crystal. Since E_{cr} is constant for all faces, a large slice energy implies a low attachment energy and therefore the face will be morphologically important. A large slice energy also implies large interactions between ions in a slice which, in turn,

* Present address: The Inorganic Chemistry Laboratory, South Parks Road, Oxford, OX1 3QR, UK

Mineralogical Magazine, December 1995, Vol. 59, pp. 607–615

means that there are at least two PBCs in the slice. This quantity has been used to predict the morphologies of a wide variety of materials (Hartman and Perdok, 1955*b*; Hartman, 1980*a*; Berkovitch-Yellin, 1985; Docherty and Roberts, 1988). The morphology derived by this methodology is known as the *growth morphology*, since it is based on the idea of layers attaching themselves to a growing crystal.

Another approach to crystal morphology is via the surface energy (the difference in energy of the surface ions to those in the bulk per unit surface area). For a crystal in equilibrium with its surroundings, the surface energy must be minimal for a given volume (Gibbs, 1928). Hence the morphological importance of a face is inversely proportional to the surface energy. The morphology derived in this way is termed the equilibrium morphology. The equilibrium morphology has been found to agree well with small experimentally grown crystals less than a micron in diameter (Hartman, 1958; Lawrence and Parker, 1990). For larger crystals and especially geological specimens, the growth morphology has been found to best reproduce the experimental results. As a result we shall limit this discussion to growth morphologies. The morphology derived by any of the methods discussed can be visualised using a Wulff plot (Wulff, 1901) with the growth rate proportional to either d_{hkl}, the attachment energy or the surface energy.

Traditionally, morphology calculations have ignored the effects of surface relaxation, i.e. the tendency of surface ions to move away from their ideal lattice sites. Although this seems a reasonable approximation for non-polar organic molecules, for inorganic systems it is known to be unrealistic. Recently, the effects of surface relaxation on the equilibrium morphology has been quantified for a few inorganic systems (Mackrodt *et al.*, 1987; Parker *et al.*, 1992). These researchers derived relaxed equilibrium morphologies and found that they were substantially different from the unrelaxed morphologies. Unfortunately they did not calculate the growth morphologies and so the effects of relaxation on them are currently unknown.

Calculation techniques

The atomistic simulations of surface relaxation presented in this work have been performed by a new surface code MARVIN (Gay and Rohl, 1995). In this program, the simulation cell many contain several blocks, with planar two-dimensional periodic boundary conditions parallel to the interface. Each block consists of two regions as shown in Fig. 1. The first contains the ions which are relaxed explicitly until there is zero force on each of them, while the ions in the second are fixed. Thus, the model of a surface consists of a block with its region 1 containing the ions closest to the surface, and the ions in region 2 are fixed to represent the potential of the remaining lattice. The methodology is closely related to that used by Tasker (1978) in the MIDAS code, but MARVIN is considerably more flexible as regards the interatomic potentials that may be used and the complexity of the systems that may be studied. MARVIN is able to calculate both equilibrium and growth morphologies both with and without surface relaxation.

The process of calculating the morphology is as follows. Firstly, the faces which are likely to appear in the morphology need to be determined so that calculations can be performed on them. These faces can be generated either by a PBC analysis (Strom, 1985) or by a Donnay-Harker analysis. We have chosen the latter, where the faces with the largest *d*-spacings are chosen, as it is easy to calculate and appears to work well. If the surfaces are going to be relaxed, it is imperative that the energy of the crystal structure of the system (bulk structure) is minimised first. Otherwise the surface calculations will be invalid as some of the surface relaxation will be minimising the strain at the region I-region II interface. These bulk minimizations have been performed using the GULP program (J.D. Gale, Royal Institution) which incorporates all the two, three and four-body potentials present in MARVIN. For each face considered, there may be more than one unique surface configuration. Each of these configurations has its unrelaxed attachment energies calculated and that with the smallest absolute attachment energy is chosen. Note that configurations with a dipole perpendicular to the surface are rejected since their surface energy is infinite (Bertaut, 1958).

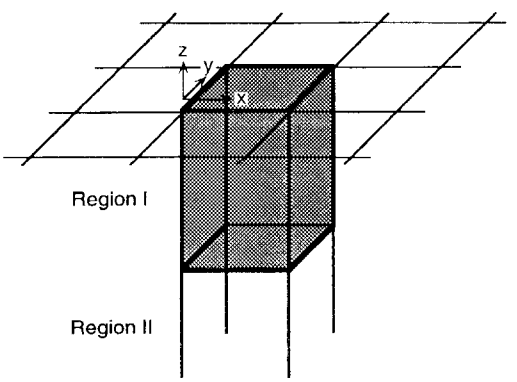

FIG. 1. Schematic of the MARVIN simulation model. The simulation cell is repeated infinitely in the x and y directions. The region I atoms are allowed to relax whilst those in region II are kept fixed.

Then the most stable surface configurations for each face are relaxed. The resulting unrelaxed and relaxed attachment energies are used to generate morphologies via the Wulff plot using the InsightII graphics package (Biosym Technologies, San Diego).

The rest of this paper is devoted to the calculated morphologies of zircon, quartz and alumina.

Zircon

Zircon was chosen to illustrate morphological calculations using MARVIN because it requires a 3-body term to describe its structure accurately and so its surfaces cannot be properly modelled using any other code. Furthermore it is composed of Zr^{4+} ions and discrete $[SiO_4]^{4-}$ molecular units, allowing the portions of the computer code applicable to complex structural units to be tested, i.e. not cleaving $[SiO_4]^{4-}$ units at the surface and using connectivity to determine the atoms between which a potential acts. Furthermore, calculations on unrelaxed surfaces of zircon exist in the literature, allowing comparison between MARVIN and other programs.

Zircon morphology

The relative morphological importance of the different faces of a mineral are given by their persistence values (P-values), i.e. the percentage of different combinations of faces in which the face has been observed. These values have been calculated by Hartman (1956) and are, in order of decreasing P-value, as follows:

{101}, {100}, {110}, {211}, {301}, {112}, {021}, {321}, {532}, {001}, {012}

Only the first two forms are F-faces. Natural zircons show a prismatic habit mostly following {100}, terminated by {101} dipyramids. However, they are sometimes observed to be prismatic following {110} with {101} dipyramids. Pupin and Turco (1981) have produced a table of zircon morphologies from a typologic study of zircon populations, in which each type of morphology is characterised by two indices, the pyramidal index A and the prismatic index T. They found that the morphology depends on temperature, and the chemistry (aluminium/alkalines ratio).

The theoretical unrelaxed morphology of zircon has been studied by Hartman (1956) and more recently by Woensdregt (1992). In the former study, the crystal was assumed to be constructed of point charges of +4 centred on the Zr lattice sites and −4 on the Si sites. In Woensdregt's study, the crystal was also composed of point charges with no short-range interactions but he considered charges centred on both the Si and O atoms of the silicate ion. He chose several different charge models to describe zircon, all with Zr^{4+} but the charge on Si ranging from +4 to 0. Both authors produced predicted morphologies which were prismatic following {100}, terminated by {101} dipyramids. The effect of reducing the charge on Si was to elongate the {100} prism. Woensdregt also calculated the morphology assuming the {101} face grew as sub-slices of {202}, since two different slices with similar attachment energies can be cut and slices of $\frac{1}{2}d_{hkl}$ at the two surfaces are both F-forms. This affected the morphology by increasing the elongation further and for the case of Si^{4+}, the {301} form appeared.

Simulation details

The potentials used here to describe zircon are an empirically derived ionic/molecular hybrid set (Gay and Rohl, 1994). In this hybrid model, which has previously been used successfully to model barium sulphate (Allan *et al.*, 1993), the silicate ion is explicitly treated as a molecular system and the potentials are of two types — *inter* (Zr−O, O−O) and *intra* (Si−O and O−Si−O). Buckingham forms were assumed for the former. For the latter, the interactions within the silicate ion were described by a Morse potential acting between Si and O and an O−Si−O three-body term. The oxygen atoms are represented by the shell model.

The surfaces with the ten largest *d*-spacings were selected as the most probable faces to appear in the morphology. The {004} was also included to ensure closure of the Wulff plot. Note that in zircon, the {103} and {321} faces have two cuts which have very similar attachment energies and so both were calculated.

TABLE 1. Attachment energies of the faces of zircon

Miller index	d_{hkl}(Å)	Attachment energy (eV mol^{-1}) unrelaxed	relaxed
(101)	4.43	−9.00	−7.25
(202)	2.22	−15.93	−7.91
(200)	3.31	−8.40	−6.36
(211)	2.65	−33.07	−33.89
(112)	2.52	−43.06	−16.64
(220)	2.34	−13.51	−15.34
(301)	2.07	−14.63	−8.70
(103)a	1.91	−52.17	−46.92
(103)b	1.91	−55.38	−27.70*
(321)a	1.76	−50.75	−66.61*
(321)b	1.76	−53.00	−48.25
(312)	1.71	−80.89	−130.04*
(213)	1.65	−39.85	−28.86
(004)	1.49	−35.64	−48.39

Simulation results

The attachment energies for the faces of zircon are listed in Table 1. The largest change upon relaxation is 41%, which occurs for the {301} face. Fig. 2 shows that this corresponds to the four Zr ions in the growth slice moving inwards, decreasing the slice energy. However, these Zr ions are now closer to the Zr ions in the layer below, increasing the repulsion between them, leading to a decrease in the attachment energy. Note that, in contrast to surface energies which must decrease upon surface relaxation, attachment energies may show an increase or decrease. Reducing the energy of region 1 during the minimization is accomplished both by moving the growth slice normal to the surface (changing E_{att}) or moving the ions within the growth slice (changing E_{slice} and E_{att}). Thus a large decrease in E_{slice} can compensate for an increase in E_{att} and *vice versa*. The relaxed attachment energies marked by an asterisk in the table are invalid since relaxation has caused ions to move out of the growth slice to the layer below or *vice versa* producing spurious results. This breakdown in the definition of attachment energy occurs only at faces with the highest unrelaxed attachment energies. The absolute values of the unrelaxed attachment energies split the faces into three groups with

$$\{200\} < \{101\} \ll \{220\} < \{301\} \ll \text{rest}$$

Relaxation has affected this ordering producing

$$\{200\} < \{101\} < \{301\} \ll \{220\} < \{112\} \ll \text{rest}$$

Note that these five forms are in the top six with smallest P-values. Thus relaxation has lowered the attachment energies of the morphologically important faces.

The calculated growth morphologies for zircon are depicted in Fig. 3. The unrelaxed growth morphologies are similar to the experimental morphology. If

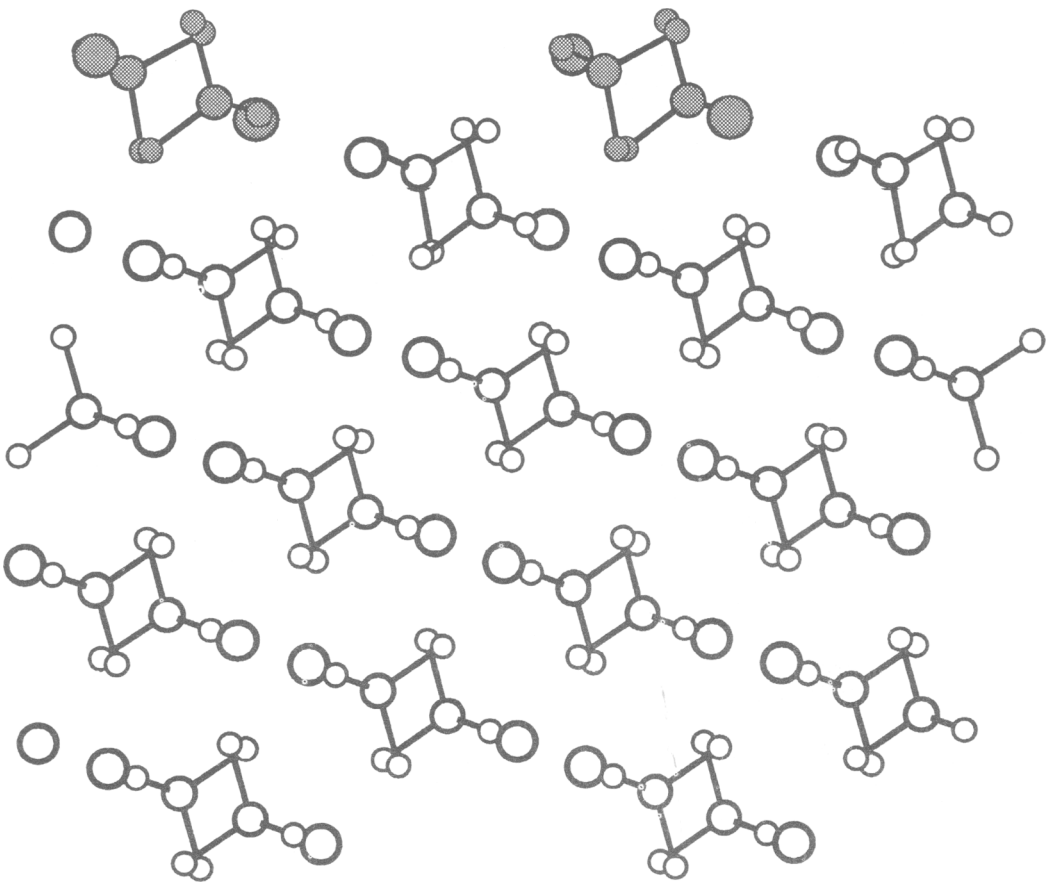

FIG. 2. The relaxed surface configuration for the (301) face of zircon. The dark ions are those in the growth slice.

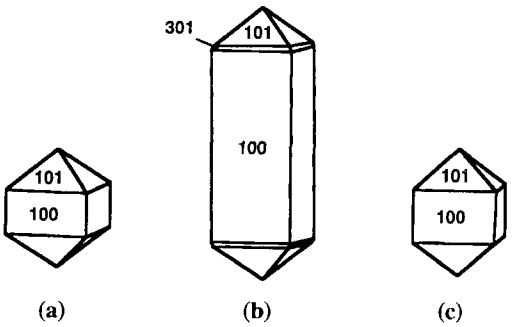

FIG. 3. Zircon morphologies. (a) unrelaxed growth morphology; (b) unrelaxed growth morphology assuming (202) growth slices; (c) relaxed growth morphology.

the growth of {101} is assumed to occur in half slices {202}, then the growth morphology becomes more elongated. The magnitude of this elongation is different from that calculated by Woensdregt. The {202} slices are polar and he calculated the attachment energy from the slice energy by Equation (1). Since the subslices are related by inversion, they are identical and have the same slice energies. However, Equation (1) does not hold for these subslices since all of the unique intermolecular interactions do not occur within the subslice or between the subslice and the bulk crystal. This can be clearly seen in Fig. 2 since the (301) face has the same properties. The (301) slice can be split into two subslices, the first of which has silicate ions immediately on either side of the boundary, the second has two zircon ions. The first does not have these Zr–Zr interactions in the slice or across the boundary, hence these interactions will be missing from the bulk energy calculated from Equation (1). The second slice will have the $[SiO_4]$–$[SiO_4]$ interactions missing. Thus there will be two different attachment energies and the one lowest in absolute value will determine the growth rate. With this one proviso, the unrelaxed growth morphology presented here compares very well with that calculated by Woensdregt (1992). The unrelaxed growth morphology corresponds to the highest A and T indices in Pupin's classification, which in turn corresponds to highest temperature growth ($\geqslant$ 900°C).

Relaxation has little effect on the growth morphology, producing only a reduction in the relative length of the prism. Relaxation does, however, have a large effect on the attachment energy of {202}, which is reduced to such an extent that it has a similar value to {101}. Thus there is little difference between the relaxed growth morphology calculated with the two different {101} growth mechanisms.

Quartz

In addition to requiring 3-body terms to describe its structure accurately, quartz has the further complication that any cleavage plane through the bulk crystal structure leads to dangling bonds at the surface. In this work, chemically plausible surfaces, generated by filling the dangling bonds with protons and hydroxyl groups, have been utilised.

Quartz morphology

The hexagonal face $\{10\bar{1}0\}$, the positive rhombohedron $\{10\bar{1}1\}$ and the negative rhombohedron $\{01\bar{1}1\}$ are almost always present on quartz crystals with the positive rhombohedron larger than the negative one. The next most important forms are the $\{\bar{2}111\}$ and $\{51\bar{6}1\}$, although they are usually quite small. However the presence of the latter is believed to be due to adsorption of foreign ions and cannot be predicted without taking these ions into account explicitly, which is beyond the scope of this paper. Hartman (1959) has demonstrated that the $\{10\bar{1}0\}$, $\{10\bar{1}1\}$ and $\{01\bar{1}1\}$ faces are F faces whilst the $\{\bar{2}111\}$ and $\{51\bar{6}1\}$ are S faces.

Simulation details

The covalent nature of quartz makes the termination of bonds broken by the creation of a surface an essential part of the simulation. It is known that silanol groups terminate typical SiO_2 surfaces in air (Hair, 1975). In this work a simple model was employed in which the bonds broken between a surface silicon and an oxygen were replaced with a hydroxide group, while the bonds between a surface oxygen and a silicon were replaced with a hydrogen, producing chemically realistic surfaces.

The potentials used in the simulation of quartz are those developed by Sanders *et al.* (1984), which were originally fitted to bulk lattice properties of α-quartz. Full ionic charges were used with the oxygen ions being represented by the shell model. These potentials have been used successfully on a wide variety of silicate systems, including zeolites (Gale and Cheetham, 1992). The SiO_2 potentials have been augmented by those of Saul *et al.* (1985), who derived the potentials for the hydroxyl group by fitting to an *ab initio* potential energy surface. Since it was found to be necessary to assign partial charges of −1.426 and +0.426 to the oxygen and hydrogen respectively, a slightly modified set of potentials (Schröder *et al.*, 1992) has been used for the interaction of the hydroxyl oxygen and the rest of the structure. In addition, a new three-body term for the silicon-oxygen-hydrogen interaction was derived from a set of *ab initio* calculations (J.D. Gale, Personal Communication).

TABLE 2. Attachment energies of the faces of quartz

Miller index	d_{hkl}(Å)	Attachment Energy (eV mol^{-1}) unrelaxed	relaxed
$(10\bar{1}0)$	4.19	−17.65	−18.56
$(10\bar{1}1)$	3.30	−19.44	−19.50
$(01\bar{1}1)$	3.30	−20.47	−20.51
$(11\bar{2}0)$	2.42	−44.98	−44.60
$(10\bar{1}2)$	2.25	−38.65	−39.54
$(01\bar{1}2)$	2.25	−41.99	−45.60
$(\bar{2}111)$	2.20	−37.74	−37.63
$(20\bar{2}1)$	1.95	−43.57	−41.57
$(02\bar{2}1)$	1.95	−82.94	−80.69
$(11\bar{2}2)$	1.79	−43.91	−42.74
(0003)	1.78	−47.56	−53.15

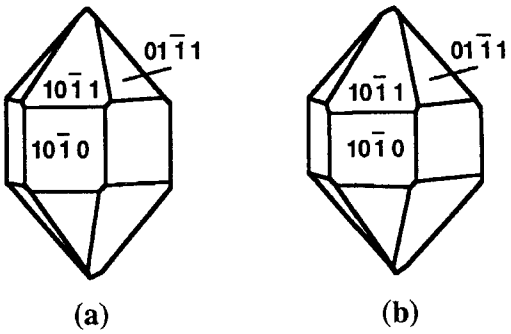

FIG. 4. Quartz morphologies. (a) unrelaxed growth morphology; (b) relaxed growth morphology.

The surfaces with the ten largest d-spacings were selected as the most probable faces to appear in the morphology. The {0003} was also included to ensure closure of the Wulff plot.

Simulation results

The data from the simulations are reported in Table 2. The unrelaxed attachment energies were calculated after the hydrogen atoms were relaxed, providing a realistic surface configuration. The relaxed energies are the energies after the energy minimization procedure discussed previously.

The Wulff plots of the quartz morphology are depicted in Fig. 4. Both growth morphologies correctly predict that the positive rhombohedron is larger than its negative counterpart. They also predict that only the hexagonal prism is also present. The effects of crystal relaxation on the attachment energies simply change the relative length of the hexagonal prism. Thus both growth morphologies agree well with observed quartz morphologies. One of the most important aspects of these simulations is that a realistic relaxed surface structure has been calculated. This is a vital prerequisite if the effects of foreign ion adsorption and chemical environment on the crystallization of quartz are to be examined.

Corundum

In the final example, we consider the morphology of corundum (α-Al_2O_3). The potential model used to describe corundum is much simpler than those for the preceding two examples and does not involve three or four-body terms, neither are any molecular mechanics forcefields required. It is of interest here though, firstly because it has previously had its growth morphology calculated without surface relaxation and it was found to disagree with experiment. Secondly, quantum mechanical calculations have been performed on the basal plane, allowing comparison with the relaxations calculated using the atomistic techniques in MARVIN.

Corundum morphology

Hartman (1980*b*) determined the theoretical growth morphology for corundum by performing a PBC analysis and calculating the attachment and surface energies for the F forms. His attachment energies were calculated for a fully ionic point charge model with Born repulsion estimated from compressibility data. No van der Waals or polarization terms were

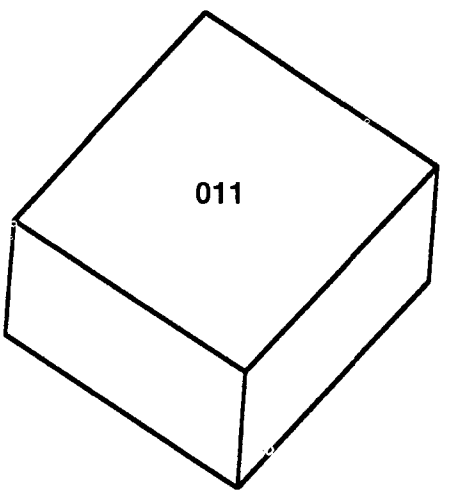

FIG. 5. Unrelaxed growth morphology of corundum calculated by Hartman (1980*b*).

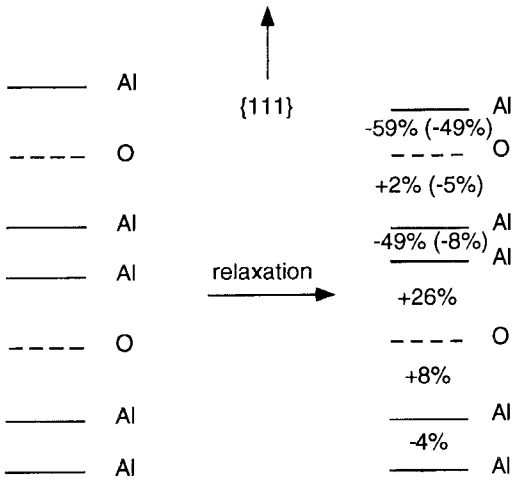

FIG. 6. Surface relaxation of the (111) face calculated by Mackrodt *et al.* (1987). The values in brackets are the relaxations calculated using a 2-D periodic *ab initio* Hartree-Fock technique (Mackrodt, 1992).

included. From Fig. 5 it can be seen that the growth morphology is dominated by {011}. Unfortunately both the synthetic (Elwell and Scheel, 1975) and natural specimens (Hartman, 1989) have {111} as the dominant form in most cases. Hartman argued that this discrepancy was a result of foreign atoms adsorbing preferentially to the (111) surface because its uppermost plane consists solely of aluminium ions with three unsaturated bonds. Mackrodt *et al.* (1987) calculated the surface relaxations for five different faces of corundum using a fully ionic model with electron gas potentials and including atomic polarization via the shell model. They demonstrated that the relaxation of the (111) face is large (see Fig. 6) and thus it becomes more stable than the (011), resulting in a dramatic effect on the equilibrium morphology. How will this relaxation affect the growth morphology?

Simulation details

Several new high quality potentials for corundum have been recently derived (Gale *et al.*, 1992), based on fitting the energy hyper surface from 3-D periodic *ab initio* Hartree-Fock calculations. We have employed the *ab initio* derived potential model (P_{qm}) which the authors designated potential 5. They actually fitted several potential models to the *ab initio* energy hypersurface for corundum. We have chosen the model which gave the smallest RMS error with no Al–Al C term in the Buckingham potential. Although incorporation of this term gave a lower RMS error, the values of the C terms obtained were unrealistic.

Calculations were performed on the twelve faces of corundum with the largest *d*-spacings. This selection includes all the faces studied by both Hartman and Mackrodt. Interestingly, the six F faces determined by Hartman correspond to the faces with the six largest *d*-spacings. This illustrates how effective the Donnay-Harker method can be when it comes to choosing faces to be analysed in a morphology calculation.

Simulation results

The calculated unrelaxed and relaxed attachment energies for the faces of corundum are presented in Table 3. The calculated unrelaxed growth morphology is identical to that found by Hartman and is dominated by {011}. As in the other cases we have considered, the attachment energies are affected by surface relaxation with an average change of 13%. The phenomenon of attachment energies increasing or decreasing on relaxation can be demonstrated by considering the (222) and (200) faces. The former exhibits an increase in the magnitude of the attachment energy whilst the latter a decrease. Each Al ion in the bulk structure of corundum is coordinated to six oxygens, half of which have a bond length of 1.86 Å and the other half 1.97 Å. At the boundary between the (222) growth slice and the bulk crystal, there are six long Al–O bonds distributed over two Al sites. During relaxation, all of these bonds decrease in length, half to 1.88 Å and the rest to 1.92 Å. Since the attachment energy is dominated by nearest neighbour interactions, which

TABLE 3. Attachment energies of the faces of corundum

Miller index	d_{hkl}(Å)	Attachment Energy (eV mol^{-1}) unrelaxed	relaxed
(011)	3.48	−2.93	−3.16
(21$\bar{1}$)	2.55	−9.52	−11.27
(10$\bar{1}$)	2.38	−5.27	−4.74
(222)	2.16	−10.90	−13.40
(210)	2.09	−10.31	−12.70
(200)	1.97	−10.24	−7.82
(321)	1.60	−14.17	−14.01
(20$\bar{1}$)	1.55	−30.37	−28.91
(21$\bar{1}$)	1.52	−33.22	−39.42
(332)	1.51	−15.05	−13.60
(31$\bar{0}$)	1.41	−22.61	−19.90
(2$\bar{1}\bar{1}$)	1.38	−18.85	−18.58

TABLE 4. Calculated relaxations for the (111) face of corundum

spacing	P_{qm}	P_{qm} only 3 layers relaxed
S_1	−51%	−47%
S_2	+6%	−2%
S_3	−55%	−12%
S_4	+22%	–
S_5	+5%	–
S_6	0%	–

are primarily Coulombic, its magnitude increases. At the (200) growth slice interface, there are again six Al−O bonds distributed over two Al sites, but two of them are short bonds. After relaxation, the short bonds are essentially unchanged; one of the long bonds has decreased to 1.86 Å, one remains unchanged and two have increased to distances of 2.47 Å and 2.31 Å. Since the combined magnitude of the expansion of two bonds is greater than single contraction, the absolute value of the attachment energy decreases.

Relaxation has had a negligible effect on the growth morphology and it is also identical to that calculated by Hartman which is shown in Fig. 5. Thus it appears likely from these calculations that the experimental morphology of corundum can only be explained by invoking an argument based on the adsorption of foreign ions at the (222) surface as postulated by Hartman.

In Table 4, the predicted relaxations of the (111) face are listed. Despite using a different potential model, these results are in excellent agreement with those of Mackrodt. These predicted relaxations though are significantly different from those calculated using the 2-D Hartree-Fock technique depicted in Fig. 6 (Mackrodt, 1992).

However this discrepancy can be accounted for when we consider that the *ab initio* calculations only allowed the three outermost atomic layers to relax. Table 4 also shows the surface structure of (111) calculated using P_{qm} subject to this restraint. Excellent agreement between the quantum mechanical and atomistic results is now obtained. This provides evidence that potentials derived from bulk calculations are valid at surfaces.

Conclusions

We have presented calculations on the morphology of zircon, quartz and corundum. The surfaces and morphology of the first two cannot be treated satisfactorily using previous morphological computer codes, since the potential parameter sets which correctly reproduce their physical properties require short-range repulsion, three-body and van der Waals terms as well as Coulombic interactions. Furthermore, quartz requires that the surface be terminated in a chemically plausible manner. The effect of surface relaxation on growth morphologies was determined for the first time. For the systems studied here, the effect was found to be small with only minor changes in the growth morphology being calculated. However, since the attachment energy can decrease or increase on relaxation, it is possible that relaxation can have a major effect on the morphology of crystals, especially those which exhibit many faces.

The unrelaxed and relaxed growth morphologies for zircon and quartz were found to be in good agreement with natural specimens but for corundum the agreement was found to be poor, even after surface relaxation. Thus, it appears that the adsorption of foreign ions at the basal plane, proposed by Hartman, is responsible for this discrepancy.

There is much debate on whether interatomic potentials derived from fitting bulk properties or quantum mechanically determined energy hypersurfaces of bulk solids are valid at surfaces. The calculated surface relaxation for the basal plane of α-Al_2O_3 was found to be in complete agreement with Hartree-Fock *ab initio* calculations. Thus it would appear that the 'bulk' potentials of alumina reproduce the interactions at low index faces. It is still not clear if these interatomic potentials will be valid at high index faces where the surface ions have low coordination numbers. Unfortunately, as yet there are no *ab initio* calculations with which to make comparisons.

The generation of realistic surfaces and their relaxation is the first step in the simulation of adsorption and diffusion of molecules on surfaces. Further MARVIN calculations will concentrate on these important physical problems, particularly the effects of adsorption of foreign ions and molecules on crystal morphology.

Acknowledgements

A.L.R. was part supported by S.E.R.C. and I.C.I. and would like to thank The Ramsay Trust and British Gas for his Ramsay Fellowship. D.H.G. would like to thank the Gas Research Institute, Chicago and Biosym Technologies, San Diego for their financial support. We are indebted to Biosym Technologies, San Diego and Cherwell Scientific, Oxford for supplying the InsightII and Ball & Stick computer codes respectively.

References

Allan, N.L., Rohl, A.L., Gay, D.H., Catlow, C.R.A., Davey, R.J. and Mackrodt, W.C. (1993) Calculated bulk and surface properties of sulphates *J. Chem. Soc. Faraday Discussions*, **95**, 273.

Berkovitch-Yellin, Z. (1985) Toward an ab initio derivation of crystal morphology. *J. Amer. Chem. Soc.*, **107**, 8239.

Bertaut, F. (1958) Physique du cristal — le terme electrostatique de l'énergie de surface. *Compt. Rendu*, **246**, 3447.

Bravais, A. (1913) *Etudes Crystallographiques*, Paris.

Docherty, R. and Roberts, K.J. (1988) Modeling the morphology of molecular crystals — application to anthracene, biphenyl and β-succinic acid. *J. Crystal Growth*, **88**, 159.

Donnay, J.D.H. and Harker, D. (1937) A new law of crystal morphology extending the law of Bravais. *Amer. Mineral.*, **22**, 446.

Elwell, D. and Scheel, M.J. (1975) *Crystal Growth from High Temperature Solutions*. Academic Press, London.

Friedel, G. (1907) Études sur la loi de Bravais. *Bull. Soc. franç. Minér.*, **30**, 326.

Gale, J.D. and Cheetham, A.K. (1992) A computer simulation of ZSM-18, *Zeolites*, **12**, 674.

Gale, J.D., Catlow, C.R.A. and Mackrodt, W.C. (1992) Periodic *ab initio* determination of interatomic potentials for alumina. *Modelling Simul. Mater. Sci. Eng.*, **1**, 73.

Gay, D.H. and Rohl, A.L. (1995) MARVIN - A new computer code for studying surfaces and interfaces and its application to calculating the crystal morphologies of corundum and zircon. *J. Chem. Soc. Farad. Trans.*, **91**, 925.

Gibbs, J.W. (1928) *Collected Works*. Longman, New York.

Hair, M.L. (1975) Hydroxyl groups on silica surface. *J. Non-Cryst. Solids*, **19**, 299.

Hartman, P. (1956) The morphology of zircon and potassium dihydrogen phosphate in relation to the crystal structure. *Acta Crystallogr.*, **9**, 721.

Hartman, P. (1958) The equilibrium forms of crystals. *Acta Crystallogr.*, **11**, 459.

Hartman, P. (1959) La morphologie structurale du quartz. *Bull. Soc. franç. Minéral Crist.*, **82**, 335.

Hartman, P. (1980*a*) The attachment energy as a habit controlling factor 2. Application to anthracene, tin tetraiodide and orthorhombic sulphur. *J. Crystal Growth*, **49**, 157.

Hartman, P. (1980*b*) The attachment energy as a habit controlling factor 3. Application to corundum. *J. Crystal. Growth*, **49**, 157.

Hartman, P. (1989) The effect of surface relaxation on crystal habit: cases of corundum (α-Al_2O_3) and hematite (α-Fe_2O_3). *J. Crystal Growth*, **96**, 667.

Hartman, P. and Bennema, P. (1980) The attachment energy as a habit controlling factor 1. Theoretical considerations. *J. Crystal Growth*, **49**, 145.

Hartman, P. and Perdok, W.G. (1955*a*) On the relationship between structure and morphology of crystals. I. *Acta Crystallogr.*, **8**, 49.

Hartman, P. and Perdok, W.G. (1955*b*) On the relationship between structure and morphology of crystals. III. *Acta Crystallogr.*, **8**, 525.

Lawrence, P.J. and Parker, S.C., (1990) Computer modelling of oxide surfaces and interfaces. In *Computer modelling of fluids, polymers and solids*. (C.R.A. Catlow *et al.*, eds.), Kluwer, Amsterdam.

Mackrodt, W.A. (1992) Classical and quantum simulation of the surface properties of α-Al_2O_3. *Phil. Trans. R. Soc. Lond.*, **A341**, 301.

Mackrodt, W.C., Davey, R.J., Black, S.N. and Docherty, R. (1987) The morphology of α-Al_2O_3 and α-Fe_2O_3: the importance of surface relaxation. *J. Crystal Growth*, **80**, 441.

Parker, S.C., Lawrence, P.J., Freeman, C.M., Levine, S.M. and Newsam, J.M. (1992) Information on catalyst surface structure from crystallite morphologies observed by scanning electron microscopy. *Catalysis Letters*, **15**, 123.

Pupin, J.P. and Turco, G. (1981) Le zircon, minéral commun significatif des roches endogènes et exogènes. *Bull. Minéral.*, **104**, 724.

Sanders, M.J., Leslie, M. and Catlow, C.R.A. (1984) Interatomic potentials for SiO_2. *J. Chem. Soc., Chem. Commun.*, 1271.

Saul, P., Catlow, C.R.A. and Kendrick, J. (1985) Theoretical studies of protons in sodium hydroxide. *J. Philos. Mag. B.*, **51**, 107.

Schröder, K.P., Sauer, J., Leslie, M., Catlow, C.R.A. and Thomas, J.M. (1992) Bridging hydroxyl groups in zeolitic catalysis — A computer simulation of their structure, vibrational properties and acidity in protonated faujasites (H-Y zeolites). *Chem. Phys. Lett.*, **188**, 320.

Strom, C.S. (1985) Finding F faces by direct chain generation. *Z. Kristallogr.*, **172**, 11.

Tasker, P.W. (1978) *A guide to MIDAS*. AERE Harwell Report R.9130.

Woensdregt, C.F. (1992) Computation of surface energies in an electrostatic point charge model: II. Application to zircon ($ZrSiO_4$). *Phys. Chem. Minerals*, **19**, 59.

Wulff, C. (1901) Zur Frage der Geschwindigkeit des Wachsthums und der Auflösung der Kristallflächen. *Z. Krystallogr.*, **34**, 449.

[*Manuscript received 15 March 1995*]